Discovery Mass Reach for Topgluons Decaying to $b\bar{b}$ at the Tevatron

Robert M. Harris
Fermilab, Batavia, IL 60510

ABSTRACT

In topcolor assisted technicolor, topgluons are massive gluons which couple mainly to top and bottom quarks. We estimate the mass reach for topgluons decaying to $b\bar{b}$ at the Tevatron as a function of integrated luminosity. The mass reach for topgluons decreases with increasing topgluon width, and is $0.77-0.95$ TeV for Run II (2 fb^{-1}) and $1.0-1.2$ TeV for TeV33 (30 fb^{-1}).

I. TOPCOLOR AND TOPGLUONS

Topcolor assisted technicolor [1] is a model of dynamical electroweak symmetry breaking in which the top quark is heavy because of a new dynamics. Topcolor replaces the $SU(3)_C$ of QCD with $SU(3)_1$ for the third quark generation and $SU(3)_2$ for the first two generations. The additional SU(3) symmetry produces a $< t\bar{t} >$ condensate which makes the top quark heavy, and gives rise to a color octet gauge boson, the topgluon B. The topgluon is expected to be wide ($\Gamma/M \approx 0.3-0.7$) and massive ($M \sim 0.5-2$ TeV). In hadron collisions it is produced through a small coupling to the first two generations, and then decays via a much larger coupling to the third generation: $q\bar{q} \rightarrow B \rightarrow b\bar{b}, t\bar{t}$. Here we estimate the mass reach for topgluons decaying to $b\bar{b}$ at the Tevatron.

II. SIGNAL

The sub-process cross section for $q\bar{q} \rightarrow b\bar{b}$ from both QCD and topgluons is given by [2]

$$\frac{d\hat{\sigma}}{d\hat{t}} = \frac{2\pi\alpha_s^2}{9\hat{s}^2}(1-\cos^2\theta^*)\left|1-\frac{\hat{s}}{\hat{s}-M^2+i\sqrt{\hat{s}}\Gamma}\right|^2 \qquad (1)$$

for a topgluon of mass M and width Γ given by

$$\Gamma = \frac{\alpha_s M}{6}\left[4\tan^2\theta + \cot^2\theta\left(1+\beta_t\left(1-\frac{m_t^2}{M^2}\right)\right)\right] \qquad (2)$$

where α_s is the strong coupling, $\hat{s}$ and $\hat{t}$ are subprocess Mandelstam variables, θ is the mixing angle between $SU(3)_1$ and $SU(3)_2$, θ^* is the scattering angle between the bottom quark and the initial state quark in the center of mass frame, $\beta_t = \sqrt{1-4m_t^2/M^2}$, and m_t is the top quark mass. Topcolor requires $\cot^2\theta >> 1$ to make the top quark heavy. In Eq. 2, the first term in square brackets is for four light quarks, and the second term has two components, the first for the bottom quark and the second for massive top quarks. In Eq. 1, the 1 inside the absolute value brackets is for the normal QCD process $q\bar{q} \rightarrow g \rightarrow b\bar{b}$. The other term inside the brackets is the Breit-Wigner topgluon resonance term for the process $q\bar{q} \rightarrow B \rightarrow b\bar{b}$. The two processes interfere constructively to the left of the mass peak and destructively to the right of the mass peak. CDF has done a preliminary search [3] in which the interference between normal gluons and topgluons was modeled in the opposite way: destructive to the left of the mass peak and constructive to the right. That model of the interference, hybrid model C in reference [4], is inappropriate for topcolor assisted technicolor and is replaced by Eq. 1. In Fig. 1 we have convoluted Eq. 1 with CTEQ2L parton distributions [5] to calculate the QCD background and topgluon signal for the case of an 800 GeV topgluon in $p\bar{p}$ collisions at $\sqrt{s} = 1.8$ TeV. Fig. 1 also includes the QCD process $gg \rightarrow b\bar{b}$ which is only significant at low mass. In Fig. 11a we plot the differential cross section $d\sigma/dm$, where m is the invariant mass of the $b\bar{b}$ system. We require both b quarks to have pseudorapidity $|\eta| < 2$ and the $b\bar{b}$ system to have center of mass scattering angle $|\cos\theta^*| < 2/3$. A clear distortion of the QCD $b\bar{b}$ spectrum is caused by the presence of a topgluon in Fig. 1a. After subtraction of the QCD background, Fig 1b shows that the signal has a very long high tail to low masses, caused by the combination of constructive interference and parton distributions that rise rapidly as the $b\bar{b}$ mass decreases. The tail is significantly larger than the peak, as seen in Fig. 1b. Nevertheless, the ratio between the topgluon signal and the QCD background, displayed in Fig. 1c, displays a noticeable peak close to the topgluon mass.

In Fig. 2 we have repeated the calculations of Fig. 1 using the PYTHIA Monte Carlo [6], including QCD radiation, and a simulation of the CDF detector. The mass peaks due to a topgluon are still visible when compared to QCD on a linear scale in Fig. 2c. Similar calculations have been performed for the masses 400, 600, and 1000 GeV.

III. BACKGROUNDS AND B-TAGGING

The QCD background we have considered so far is only the lowest order processes $q\bar{q} \rightarrow b\bar{b}$ and $gg \rightarrow b\bar{b}$. For an analysis in which we only tag one of the two b quarks, the background should also includes contributions from final state gluon splitting to $b\bar{b}$, flavor excitation where an initial state gluon splits into $b\bar{b}$ and one of the two b quarks undergoes a hard scatter, and contributions from jets faking a b-tag and from charm. To get the most realistic estimate of the background we use CDF run 1A data in which we require at least one of the two leading jets to be tagged as a bottom quark. The b-tag requires a displaced vertex in the secondary vertex detector [7]. The $b\bar{b}$ reconstruction efficiency when we required at least a single b-tag was 0.25 in run 1A [3]. In Fig. 2d we show CDF run 1A data on both the untagged dijet mass spectrum and the b-tagged dijet mass spectrum compared to a parameterized fit [3]. Notice that the single b-tagged dijet mass spectrum is about an order of magnitude higher than the simulated background from direct $b\bar{b}$ in Fig. 2a.

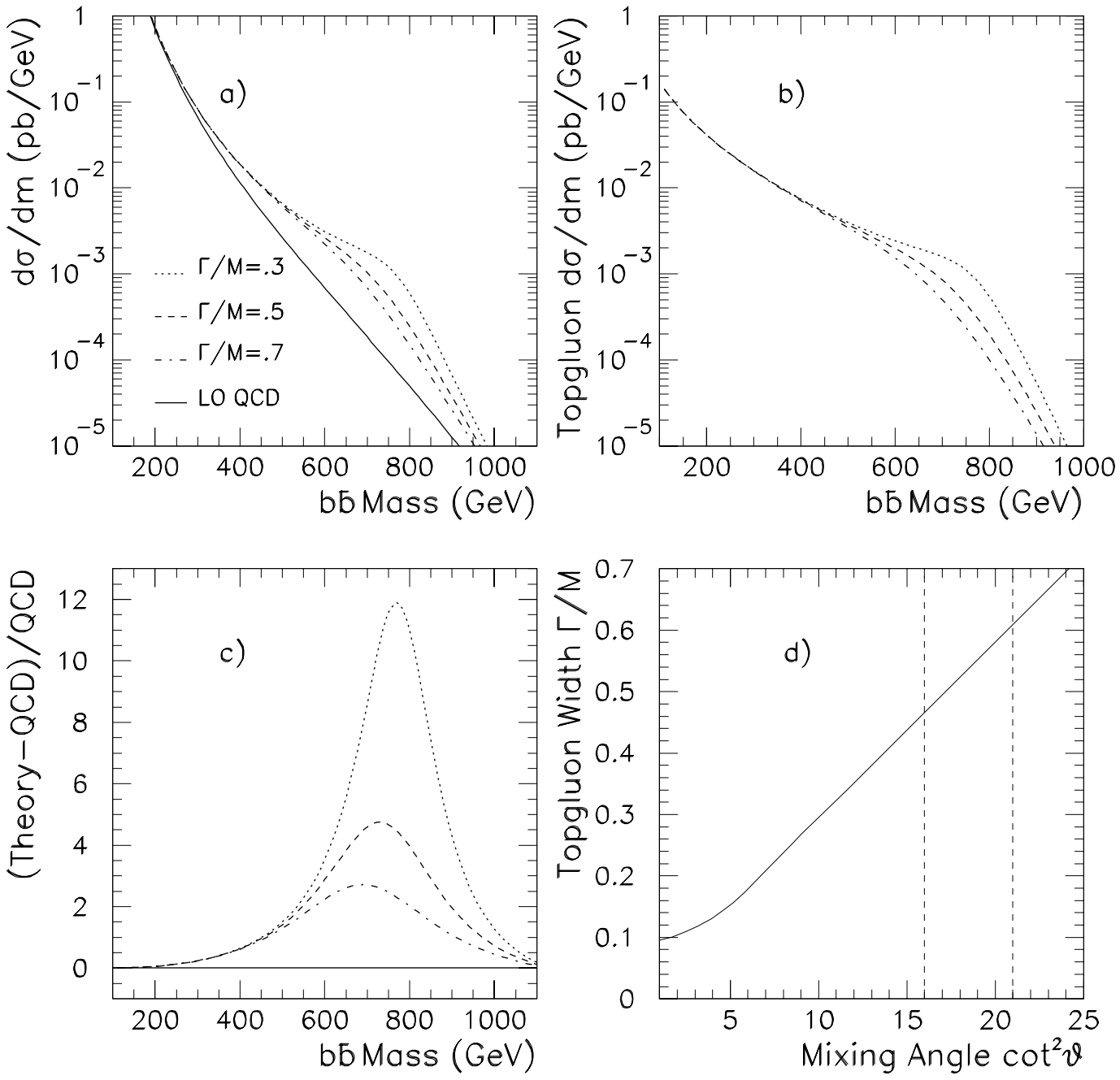

Figure 1: Lowest order parton level predictions for an 800 GeV topgluon decaying to $b\bar{b}$ displayed as a function of $b\bar{b}$ mass. a) The cross section for the LO $b\bar{b}$ background from QCD (solid) is compared to the coherent sum of LO QCD and a topgluon of fractional width $\Gamma/M = 0.3$ (dots), 0.5 (dashes) and 0.7 (dotdash). In b) the QCD prediction has been subtracted leaving only the topgluon signal and the interference between QCD and topgluons (constructive beneath peak, destructive above peak). c) The fractional deviation above the QCD prediction produced by the presence of a topgluon. d) The solid curves give the topgluon width as a function of the mixing angle between $SU(3)_1$ and $SU(3)_2$ for an 800 GeV topgluon. The vertical dashed lines indicate the theoretically preferred range of mixing angle [8].

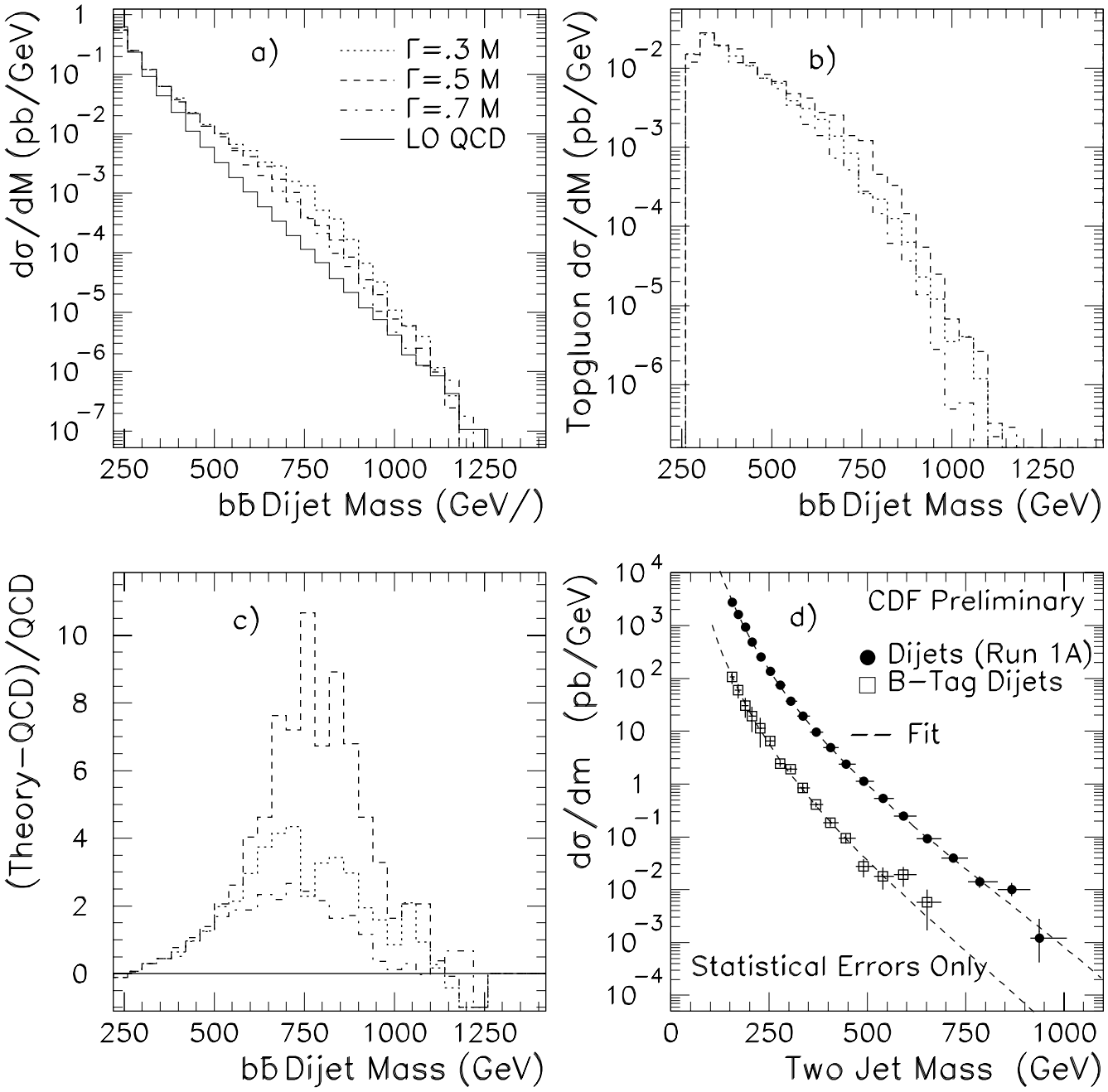

Figure 2: Simulation of an 800 GeV topgluon and measurement of background in the CDF detector. a), b) and c) are the same as in Fig. 1 except they include QCD radiation from PYTHIA and a CDF detector simulation. d) Dijet mass data (solid points) and b-tagged dijet mass data (open boxes) both from run 1A only, are compared to a parameterized fit to the data (curve).

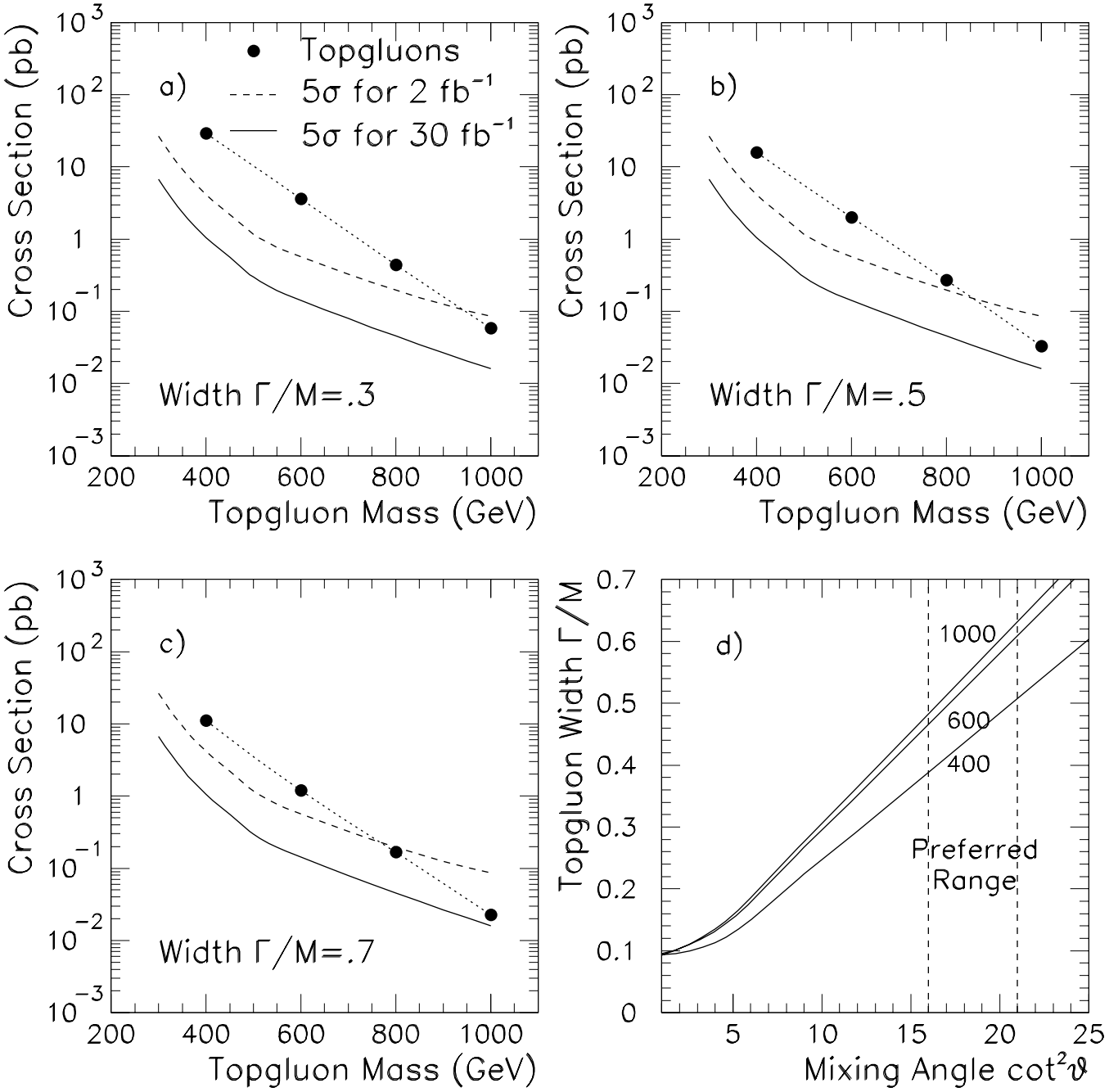

Figure 3: The mass reach for $b\bar{b}$ decays of topgluons of width a) 0.3 M, b) 0.5 M, and c) 0.7 M. The predicted cross section for topgluons (points) is compared to the 5σ discovery reach of the Tevatron with a luminosity of 2 fb^{-1} (dashed) and 30 fb^{-1} (solid). All cross sections are for $b\bar{b}$ with $|\eta| < 2$, $|\cos\theta^*| < 2/3$, and invariant mass within 25% of the topgluon peak. d) The solid curves give the topgluon width as a function of the mixing angle between $SU(3)_1$ and $SU(3)_2$ for 3 different topgluon masses. The vertical dashed lines indicate the theoretically preferred range of mixing angle [8].

We estimate that the single b-tagged data is roughly 20% fakes, 30% charm, 50% bottom, and only 1/5 of the bottom component is direct $b\bar{b}$ and the rest is gluon splitting and flavor excitation [3]. We fit the b-tagged dijet mass spectrum to the functional form, $d\sigma/dm = A(1 - m/\sqrt{s})^N/m^p$, with parameters A, N and p. The fit is used to estimate the background to topgluons when calculating the discovery reach.

IV. DISCOVERY MASS REACH

To calculate the discovery mass reach we integrate both the fully simulated topgluon signal cross section and the b-tagged dijet background parameterization within the range $0.75M < m < 1.25M$. The resulting total topgluon signal in the $b\bar{b}$ channel is shown in Fig. 3. The resulting background rate in this mass range is used to find the 5 σ discovery cross section. This is conservatively defined as the cross section which is above the background by 5 σ, where σ is the statistical error on the measured cross section (not the background). For example, if the background were zero events the 5σ discovery rate would be 25 events. To obtain the discovery cross section we used both the luminosity and the 25% $b\bar{b}$ reconstruction efficiency. In Fig. 3 we compare the topgluon signal cross section to the 5 σ discovery cross section for two different luminosities: 2 fb^{-1} for Tevatron collider run II and 30 fb^{-1} for TeV33. The topgluon discovery mass reach, defined as the mass at which a topgluon would be discovered with a 5σ signal, is tabulated in Table I as a function of integrated luminosity and topgluon width. The mass reach decreases with increasing width, caused by worsening signal to background within the search window. The width as a function of mixing angle, from Eq. 2, is shown in Figs. 1d and 3d. Also shown is the preferred theoretical range for the mixing angle $\cot^2\theta$, determined from the topcolor model and constraints from other data [8], which then implies an allowed width of the topgluon somewhere in the range $\Gamma/M \approx 0.3 - 0.7$.

V. SYSTEMATICS AND IMPROVEMENTS

In this analysis, we have not included any systematic uncertainties on the measured signal, and we have assumed that the shape and magnitude of the single b-tagged background spectrum will be well understood. Also, we have approximated the background by an extrapolation of existing b-tagged data into a higher mass region. Adding systematics on the signal and the background will decrease the mass reach of a real search. However, we anticipate a factor of two improvement in b-tagging efficiency when the run 1B algorithm is used, and further improvements are possible in Run II and TeV33. Also, this analysis only considers single b-tagging; an analysis which tags both b quarks from the topgluon decay will likely have a significantly better discovery reach because the backgrounds from gluon splitting, flavor excitation, and fakes will be significantly reduced. In order to have a background estimate from the data, we did the analysis for a center of mass energy of $\sqrt{s} = 1.8$ TeV, while Run II and TeV33 will be at $\sqrt{s} = 2.0$ TeV which could provide a 10% larger mass reach. We have also not done a maximum likelihood fit, which would be a more sensitive statistical test for the presence of a signal. Adding these improvements should increase the mass reach of a real search. The positive consequences of future improvements will likely exceed the negative consequences of neglecting systematics. We believe our analysis gives a conservative estimate of the mass reach.

Table I: The 5σ discovery mass reach of the Tevatron in Run II (2 fb^{-1}) and TeV33 (30 fb^{-1}) for a toplguon decaying to $b\bar{b}$ as a function of its fractional width (Γ/M).

Width	Mass Reach	
Γ/M	2 fb^{-1}	30 fb^{-1}
0.3	0.95 TeV	1.2 TeV
0.5	0.86 TeV	1.1 TeV
0.7	0.77 TeV	1.0 TeV

VI. SUMMARY AND CONCLUSIONS

We have used a full simulation of topgluon production and decay to $b\bar{b}$, and an extrapolation of the b-tagged dijet mass data [3], to estimate the topgluon discovery mass reach in a $b\bar{b}$ resonance search. The topgluon discovery mass reach, $0.77 - 0.95$ TeV for Run II and $1.0 - 1.2$ TeV for TeV33, covers a significant part of the expected mass range ($\sim 0.5 - 2$ TeV). For comparison, the mass reach in the $t\bar{t}$ channel is estimated to be $1.0-1.1$ TeV for Run II and $1.3-1.4$ TeV for TeV33 [9]. This is greater than the mass reach in the $b\bar{b}$ channel primarily because of smaller $t\bar{t}$ backgrounds. If topgluons exist, there is a good chance we will find them at the Tevatron, beginning the investigation into the origins of electroweak symmetry breaking.

VII. REFERENCES

[1] C. Hill, Phys. Lett. **B345**, 483 (1995).

[2] K. Lane, BUHEP-96-8, hep-ph/9605257, and these proceedings.

[3] R. Harris (CDF Collaboration), hep-ex/9506008, Fermilab-conf-95/152-E.

[4] C. Hill and S. Parke, Phys. Rev. **D49**, 4454 (1994).

[5] J. Botts *et al.*, Phys. Lett. **B304**, 159 (1993).

[6] T. Sjostrand, computer code PYTHIA V5.6, CERN-TH-6488/92.

[7] F. Abe *et al.* (CDF), Phys. Rev **D50**, 2966 (1994).

[8] G. Buchalla, G. Burdman, C. Hill and D. Kominis, Phys. Rev. **D53**, 5185 (1996).

[9] R. Harris, Fermilab-Conf-96/277-E, and these proceedings.